



## Original

# miR-145-5p attenuates inflammatory response and apoptosis in myocardial ischemia-reperfusion injury by inhibiting (NADPH) oxidase homolog 1

Lili TAN<sup>1</sup>\*, Limin LIU<sup>1</sup>\*, Jian YAO<sup>2</sup>) and Chenghao PIAO<sup>1</sup>)

<sup>1</sup>)Department of Cardiology, The Second Affiliated Hospital of Shenyang Medical College, 20 Beijiu Road, Shenyang 110002, P.R. China

<sup>2</sup>)Department of Cardiovascular Surgery, The Second Affiliated Hospital of Shenyang Medical College, 20 Beijiu Road, Shenyang 110002, P.R. China

**Abstract:** Myocardial ischemia-reperfusion (I/R) injury is a common complication following reperfusion therapy that involves a series of immune or apoptotic reactions. Studies have revealed the potential roles of miRNAs in I/R injury. Herein, we established a myocardial I/R model in rats and a hypoxia/reoxygenation (H/R) model in H9c2 cells and investigated the effect of miR-145-5p on myocardial I/R injury. After 3 h or 24 h of reperfusion, left ventricular end-systolic pressure (LVESP), ejection fraction (EF), and fractional shortening (FS) were obviously decreased, and left ventricular end-diastolic pressure (LVEDP) was increased. Meanwhile, I/R induced an increase in myocardial infarction area. Moreover, a decrease in miR-145-5p and increase in (NADPH) oxidase homolog 1 (NOH-1) were observed following I/R injury. With this in mind, we performed a luciferase reporter assay and demonstrated that miR-145-5p directly bound to NOH-1 3' untranslated region (UTR). Furthermore, miR-145-5p mimics decreased the levels of tumor necrosis factor (TNF)- $\alpha$ , IL-1 $\beta$ , and IL-6 via oxygen and glucose deprivation/reperfusion (OGD/R) stimulation. Upregulation of miR-145-5p increased cell viability and reduced apoptosis accompanied by downregulation of Bax, cleaved caspase-3, cleaved poly(ADP-ribose) polymerase (PARP) and upregulation of Bcl2. In addition, miR-145-5p overexpression increased superoxide dismutase (SOD) activity and reduced reactive oxygen species (ROS) and malondialdehyde (MDA) content under OGD/R stress. Notably, NOH-1 could significantly abrogate the above effects, suggesting that it is involved in miR-145-5p-regulated I/R injury. In summary, our findings indicated that miR-145-5p/NOH-1 has a protective effect on myocardial I/R injury by inhibiting the inflammatory response and apoptosis.

**Key words:** apoptosis, inflammatory response, miR-145-5p, myocardial ischemia-reperfusion injury, (NADPH) oxidase homolog 1 (NOH-1)

## Introduction

Acute myocardial infarction (AMI) is a common cardiovascular disease with a high incidence of morbidity and mortality in the world [1, 2]. At present, there are several potential treatments applied for AMI, such as thrombolytic therapy, percutaneous coronary intervention, and coronary artery bypass grafting [3]. However,

reperfusion after ischemia is likely to exacerbate myocardial dysfunction, leading to irreversible tissue damage, which is also called myocardial ischemia-reperfusion (I/R) injury [4]. Recent studies have shown that myocardial I/R injury is a complicated and multifactorial pathological process involving a series of biological alterations, including mitochondrial dysfunction, inflammation, myocardial cell apoptosis, and necrosis [5, 6].

(Received 5 November 2020 / Accepted 26 January 2021 / Published online in J-STAGE 4 March 2021)

Corresponding author: L. Tan. e-mail: tanlili123@163.com

\*These authors contributed equally to this study.

Supplementary Figure: refer to J-STAGE: <https://www.jstage.jst.go.jp/browse/expanim>



This is an open-access article distributed under the terms of the Creative Commons Attribution Non-Commercial No Derivatives (by-nc-nd) License <<http://creativecommons.org/licenses/by-nc-nd/4.0/>>.

Therefore, how I/R-induced myocardial dysfunction can be alleviated is of great significance for the development of treatment strategies for ischemic heart disease.

(NADPH) oxidase homolog 1 (NOH-1) belongs to a family of transmembrane proteins with wide involvement in the pathogenesis of cardiac dysfunction [7, 8]. NOH-1 represents the main NADPH oxidase isoform responsible for superoxide production and plays an important role in the regulation of inflammation and apoptosis [8–10]. It promotes norepinephrine-induced reactive oxygen species (ROS) production in the heart [11]. Knockdown of NOH-1 prevents against cobalt chloride (CoCl<sub>2</sub>)-induced hypoxic injury, which is accompanied by increased endogenous antioxidant enzyme activity and activation of protective autophagy in cardiac H9c2 cells [12]. NOH-1 can also activate the inflammatory response induced by the pro-inflammatory factor tumor necrosis factor (TNF)- $\alpha$ , along with a large amount of pro-inflammatory cytokine secretion in vascular smooth muscle cells [13]. On the other hand, loss of NOH-1 attenuates the inflammatory response and contributes to hypertensive cardiac remodelling [14]. Notably, NOH-1 has been reported to be highly expressed in cardiomyocytes and cardiac tissue [15]. Nevertheless, the role of NOH-1 in myocardial I/R injury and its molecular mechanism are elusive.

MicroRNAs (miRNAs) are small non-coding RNAs of 19 to 25 nucleotides that play important regulatory roles in processes involved in the development and progression of cardiovascular diseases, including heart development, myocardial apoptosis, and cardiac hypertrophy [16, 17]. In previous studies, researchers have demonstrated that miR-145-5p can improve myocardial I/R injury, which is correlated with alleviation of the inflammatory response and apoptosis during the development of ischemia injury [18, 19]. Conversely, miR-145-5p has also been found to promote I/R-induced apoptosis in cardiomyocytes and rat models [20]. In this study, a bioinformatics analysis showed that miR-145-5p has targeted binding sites on the 3'-untranslated region of NOH-1. However, further study is required to determine whether the role of miR-145-5p in I/R is achieved by modulating NOH-1.

In the present study, an *in vivo* model of I/R in rats and an *in vitro* model of oxygen and glucose deprivation/reperfusion (OGD/R) in H9c2 cells were established, and we investigated the effect of miR-145-5p/NOH-1 on myocardial ischemic injury and the potential mechanisms.

## Materials and Methods

### I/R injury model in rats

The study was approved by the Animal Care and Use Committee of The Second Affiliated Hospital of Shenyang Medical College (Shenyang, China). The animal license number was SYYXY2019031501. Male Sprague Dawley (SD) rats aged 10 weeks were kept under a constant temperature conditions with a 12 h light/12 h dark cycle and free access to food and water. Rats were randomly divided into four groups (n=6 in each group): Sham 3 h, I/R 3 h, Sham 24 h, and I/R 24 h. As described by Yang *et al.* [21], the heart was exposed through a left thoracotomy, and the Left anterior descending coronary artery (LAD) was ligated for 30 min. After 30 min of ischemia, the rats were subjected to 3 h and 24 h of reperfusion. The rats in the Sham groups received the same procedure without LAD artery occlusion.

### Detection of cardiac function

After 3 h and 24 h reperfusion, echocardiography was performed to measure left ventricular end-systolic pressure (LVESP), left ventricular end-diastolic pressure (LVEDP), ejection fraction (EF) and fractional shortening (FS).

### Infarct size measurement

The infarct size was determined in collected hearts using triphenyltetrazolium chloride (TTC) staining (Solarbio, Beijing, China). The samples were cut into slices and stained with 1% TTC for 10–15 min at 37°C. The red area was identified as the area at risk (AAR), while unstained (white) area was identified as the infarct area (IA). The AAR and IA were measured by computerized planimetry. The IA/AAR ratio was then calculated.

### Cell culture and transfection

H9c2 cell lines were purchased from Procell Life Science & Technology Co., Ltd. (Wuhan, China) and cultured in DMEM medium (Procell, Wuhan, China) supplemented with 10% fetal bovine serum (FBS; Sigma, St. Louis, MO, USA) at 37°C in an atmosphere containing 5% CO<sub>2</sub>. For miR-145-5p overexpression or suppression, miR-145-5p mimics, negative control (NC) mimics, miR-145-5p inhibitors, or NC inhibitors were transfected into H9c2 cells. The sequences of the miR-145-5p mimics, NC mimics, miR-145-5p inhibitors, and NC inhibitors (JTS Scientific, Wuhan, China) were as follows: 5'-GUCCAGUUUCCAGGAAUCCCU-3' (sense) and 5'-GGAUCCUGGGAAAACUGGACUU-3' (antisense) for miR-145-5p mimics, 5'-UU-

CUCCGAACGUGUCACGUTT-3' (sense) and 5'-ACGUGACACGUUCGGAGAATT-3' (antisense) for NC mimics, 5'-AGGGAUUCUGGGAAAACUGGAC-3' for miR-145-5p inhibitors, and 5'-UUGUACUACACAAAAGUACUG-3' for NC inhibitors. Furthermore, to evaluate the effects of NOH-1 and miR-145-5p, an NOH-1-overexpressing plasmid or empty vector and miR-145-5p mimics or NC mimics were co-transfected into H9c2 cells. All transfections were performed using Lipofectamine 3000 Reagent (Gibco, New York, NY, USA) according to the manufacturer's protocols. Transfection efficiency was measured by qRT-PCR or western blot analysis.

### Oxygen and glucose deprivation/reperfusion (OGD/R) model in H9c2 cells

After co-transfection of miR-145-5p mimics and the NOH-1-overexpressing plasmid for 48 h, H9c2 cells were cultured in glucose-free DMEM in an anaerobic chamber (95% N<sub>2</sub>, 5% CO<sub>2</sub>) at 37°C for 6 h. After exposure to hypoxia, the cells were maintained in a glucose-containing medium with 95% air and 5% CO<sub>2</sub> for 18 h to allow them to recover.

### Luciferase reporter assay

HEK-293T cells were co-transfected with 3' UTR of wild-type (WT) or mutant (Mut 1 and 2) NOH-1 and miR-145-5p mimics or NC mimics using Lipofectamine 3000. After transfection for 48 h, the cells were harvested and lysed. Relative luciferase activity was determined with a luciferase assay kit (Promega, Madison, WI, USA) according to the manufacturer's instructions.

### Quantitative real-time PCR (qRT-PCR)

Total RNA from myocardial tissues and H9c2 cells was isolated with TRIzol reagent (Tiangen, Beijing, China) and converted into cDNA using reverse transcriptase (Tiangen, Beijing, China). The relative expression levels of miR-145-5p, NOH-1, TNF- $\alpha$ , IL-1 $\beta$ , and IL-6 were determined using a SYBR Green-based qRT-PCR assay (Solarbio) with the relevant primers. Expression of 5S or glyceraldehyde-3-phosphate dehydrogenase (GAPDH) served as the internal reference. The sequences of all the PCR primers (GenScript, Nanjing, China) were as follows: 5'-GTCCAGTTTTCCAGGAATCC-3' (forward) and 5'-GCAGGGTCCGAGGTATTC-3' (reverse) for miR-145-5p, 5'-GATCTCGAAGCATAAAGCAGG-3' (forward) and 5'-TGGTGCAGGGTCCGAGGTAT-3' (reverse) for 5S, 5'-TTTCCTAAACTACCGACTCTTCC-3' (forward) and 5'-TTGTCCCAATTGGTCTCCC-3' (reverse) for NOH-1, 5'-CG-

GAAAGCATGATCCGAGAT-3' (forward) and 5'-AGACAGAAGAGCGTGGTGGC-3' (reverse) for TNF- $\alpha$ , 5'-TTCAAATCTCACAGCAGCAT-3' (forward) and 5'-CACGGGCAAGACATAGGTAG-3' (reverse) for IL-1 $\beta$ , 5'-AACTCCATCTGCCCTTCA-3' (forward) and 5'-CTGTTGTGGGTGGTATCCTC-3' (reverse) for IL-6, and 5'-CGGCAAGTTCAACGGCACAG-3' (forward) and 5'-CGCCAGTAGACTCCACGACAT-3' (reverse) for GAPDH.

### Western blot

Total protein was extracted using radioimmunoprecipitation assay (RIPA; Solarbio) buffer and phenylmethanesulfonyl fluoride (PMSF; Solarbio) and then quantified with a BCA Protein Analysis kit (Solarbio). The protein extracted was subsequently separated by sodium dodecyl sulfate polyacrylamide gel electrophoresis (SDS-PAGE; Solarbio) and then transferred onto polyvinylidene fluoride (PVDF) membranes (Millipore, Billerica, MA, USA). After blocking in 5% nonfat milk, the membranes were incubated with specific primary antibodies against NOH-1 (Abcam, Cambridge, UK), TNF- $\alpha$  (Abcam), IL-1 $\beta$  (ABclonal, Wuhan, China), IL-6 (Affinity, China), Bax (CST, Boston, MA, USA), Bcl2 (Abcam), caspase-3 (CST), poly(ADP-ribose) polymerase (PARP) (CST) and GAPDH (Proteintech, Wuhan, China) at 4°C overnight. These membranes were then incubated with horseradish peroxidase-labeled IgG (IgG-HRP; Solarbio) for 1 h at 37°C, and the bands were visualized using enhanced chemiluminescence (ECL; Solarbio) detection systems. Analysis of the gray values for proteins was conducted with the ImageJ software.

### MTT (3-(4,5-dimethylthiazol-2-yl)-2,5-diphenyltetrazolium bromide) assay

At 48 h post-transfection, H9c2 cells were harvested at a density of  $4 \times 10^3$  cells/well. Cell viability was determined using an MTT assay kit (Beyotime, Shanghai, China) according to the instructions of the manufacturer. The optical density (OD) value was measured at 570 nm with a microplate reader (BioTek, Winooski, VT, USA).

### Terminal deoxynucleotidyl transferase (TdT) dUTP nick-end labeling (TUNEL) assay

TUNEL staining was performed with an In Situ Cell Death Detection Kit (Roche, Basel, Switzerland), according to the manufacturer's protocol, to determine the number of apoptotic cardiomyocytes. H9c2 cells were fixed with 0.1% Triton X-100 (Beyotime) for 15 min at room temperature. After washing with phosphate buffer solution (PBS; Sangon, Shanghai, China) 3 times, the

sections were incubated with TUNEL reaction mixture in the dark at 37°C for 1 h. After that, the sections were incubated with DAPI (Aladdin, Shanghai, China) for 5 min and washed 3 times with PBS. The number of apoptotic cardiomyocytes was observed under a microscope (Olympus, Tokyo, Japan) at a magnification of 400×.

### ROS detection by flow cytometry

H9c2 cells were collected and washed twice in PBS. After centrifugation at 140 g for 5 min, the cells were incubated with DCFH-DA (Keygen, Nanjing, China) at 37°C for 30 min. After that, the cells were washed 3 times in PBS, and the ROS production was examined using a flow cytometer (ACEA Biosciences, San Diego, CA, USA).

### Detection of superoxide dismutase (SOD) activity

The activity of the anti-oxidative enzyme SOD was detected using an SOD Activity Assay Kit according to the manufacturer's instructions (Nanjing Jiancheng, Nanjing, China). The specific binding optical density was measured at 550 nm with a microplate reader (BioTek).

### Detection of malondialdehyde (MDA) concentration

The concentration of the oxidative stress product MDA was monitored with an MDA Assay Kit (Nanjing Jiancheng). Absorbance was visualized at 532 nm with a microplate reader (BioTek).

### Statistical analysis

Data were analyzed using the GraphPad Prism 8 software and presented as the mean ± SD. Comparisons of data between two groups were assessed using Student's *t*-test. Differences among multiple groups were examined using analysis of variance (ANOVA), followed by Tukey's multiple comparisons as post hoc tests. A *P*-value <0.05 was considered statistically significant.

## Results

### miR-145-5p expression decreased and NOH-1 increased in the I/R model

Rats were subjected to ischemia for 30 min followed by reperfusion for 3 h or 24 h. Subsequently, we demonstrated that LVESP, EF, and FS were obviously decreased and that LVEDP was increased in rats of the I/R group (Figs. 1A–D). The results of TTC staining suggested that I/R injury resulted in a significant increase in infarct size in the I/R groups (Figs. 1E and F). Moreover, miR-145-5p and NOH-1 expression levels were significantly downregulated and upregulated, respec-

tively, in response to I/R injury (Figs. 1G and H), indicating that miR-145-5p/NOH-1 may play a critical role in I/R injury.

### NOH-1 is a target of miR-145-5p

The miRDB online prediction database indicated that miR-145-5p had two putative target binding sites on NOH-1 3' UTR (Fig. 2A). To confirm this prediction, a luciferase reporter assay was performed. Overexpression of miR-145-5p with mimics induced a reduction in the luciferase activity of NOH-1 3' UTR WT, while it had no impact on the mutant type (Fig. 2B), indicating interaction between NOH-1 and miR-145-5p. In addition, we transfected miR-145-5p mimics, NC mimics, miR-145-5p inhibitors or NC inhibitors into H9c2 cells and found that miR-145-5p expression was increased by miR-145-5p mimics but decreased by miR-145-5p inhibitors (Fig. 2C). More importantly, overexpression of miR-145-5p significantly reduced NOH-1 expression, whereas silencing of miR-145-5p increased it (Figs. 2D and E), suggesting that NOH-1 expression can be regulated by miR-145-5p. These results imply that miR-145-5p and NOH-1 may have some regulatory roles in I/R development.

### Effect of NOH-1 on OGD/R-induced inflammatory response

As illustrated in Fig. 3A, transfection with the NOH-1-overexpressing plasmid induced an elevation in NOH-1 expression. After OGD/R induction, the mRNA and protein levels of TNF- $\alpha$ , IL-1 $\beta$ , and IL-6 were increased. MiR-145-5p reduced the expression of these inflammatory cytokines, and this was reversed by overexpression of NOH-1 (Figs. 3B–G). These findings demonstrate that NOH-1 contributes to the inflammatory response of OGD/R-induced H9c2 cells, which may be mediated by miR-145-5p.

### Effect of NOH-1 on OGD/R-induced apoptosis

The MTT assay showed that miR-145-5p increased cell viability inhibited by OGD/R, whereas cell viability was reduced after transfection with the NOH-1-overexpressing plasmid (Fig. 4A). We further evaluated the effect of NOH-1 on apoptosis of OGD/R-induced H9c2 cells, as shown in Figs. 4B and C. Overexpression of miR-145-5p decreased the OGD/R-induced cell apoptosis rate, along with the elevation of Bax, cleaved caspase-3, and cleaved PARP and the reduction of Bcl2. Notably, these above effects were abrogated by NOH-1 upregulation. In addition, miR-145-5p decreased the generation of ROS and MDA and increased SOD activity induced by OGD/R stimulation, which was also

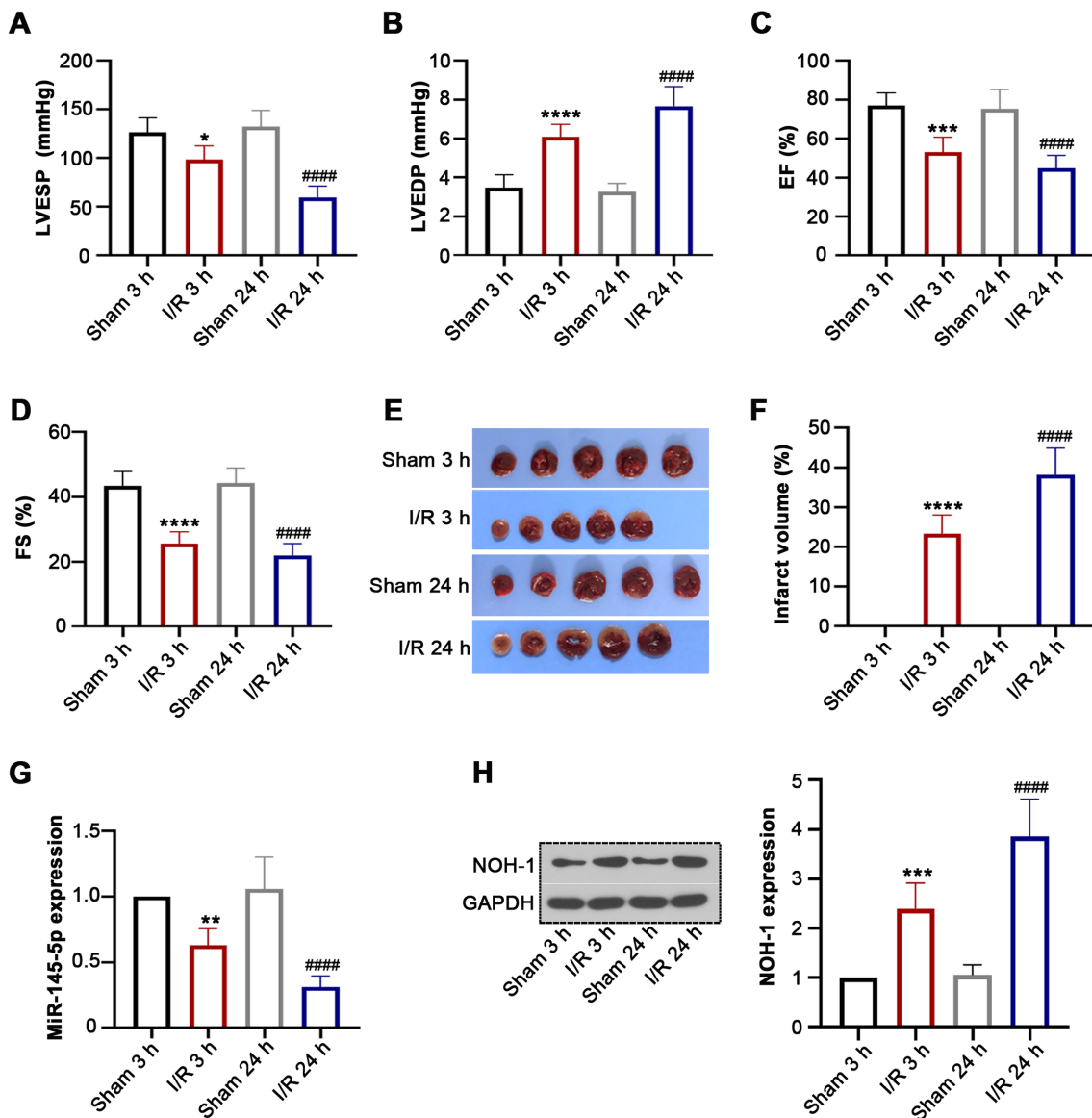


**Fig. 1.** (NADPH) oxidase homolog 1 (NOH-1) expression was increased in rats with ischemia reperfusion (I/R) injury. Healthy male Sprague Dawley (SD) rats were divided into Sham 3 h, I/R 3 h, Sham 24 h, and I/R 24 h groups (n=6 per group). They were then subjected to oxygen and glucose deprivation for 30 min followed by reperfusion for 3 h and 24 h. (A–D) At 3 h and 24 h post-reperfusion, the indicators related to cardiac function, including left ventricular end-systolic pressure (LVESP), left ventricular end-diastolic pressure (LVEDP), ejection fraction (EF), and fractional shortening (FS), were measured using echocardiography. (E) The infarct regions were determined by triphenyltetrazolium chloride (TTC) staining. (F) The infarct volumes were analyzed using the ImageJ software. (G) Relative expression of miR-145-5p was detected by qRT-PCR. (H) NOH-1 protein expression was determined using western blot analysis. All results are presented as means  $\pm$  SD from six independent experiments, and they were analyzed by one-way ANOVA. \* $P$ <0.05, compared with the Sham 3 h group. \*\*  $P$ <0.01, compared with the Sham 3 h group. \*\*\*  $P$ <0.001, compared with the Sham 3 h group. \*\*\*\*  $P$ <0.0001, compared with the Sham 3 h group. ####  $P$ <0.0001, compared with the Sham 24 h group.

abolished by NOH-1 (Figs. 5A–C). Collectively, these results indicated the anti-apoptotic and anti-oxidative effects of miR-145-5p/NOH-1 on IR injury.

## Discussion

Although investigators have revealed the function of miR-145-5p in the process of myocardial I/R injury, whether miR-145-5p functions by modulating NOH-1

is not entirely understood. In the present study, we demonstrated that miR-145-5p suppressed the release of pro-inflammatory cytokines TNF- $\alpha$ , IL-1 $\beta$ , and IL-6 and reduced apoptosis and oxidative stress induced by OGD/R and that these effects were in turn reversed by NOH-1 upregulation, as illustrated in Supplementary Fig. 1.

In our *in vivo* experiment, we successfully established a rat model of myocardial I/R injury. After reperfusion

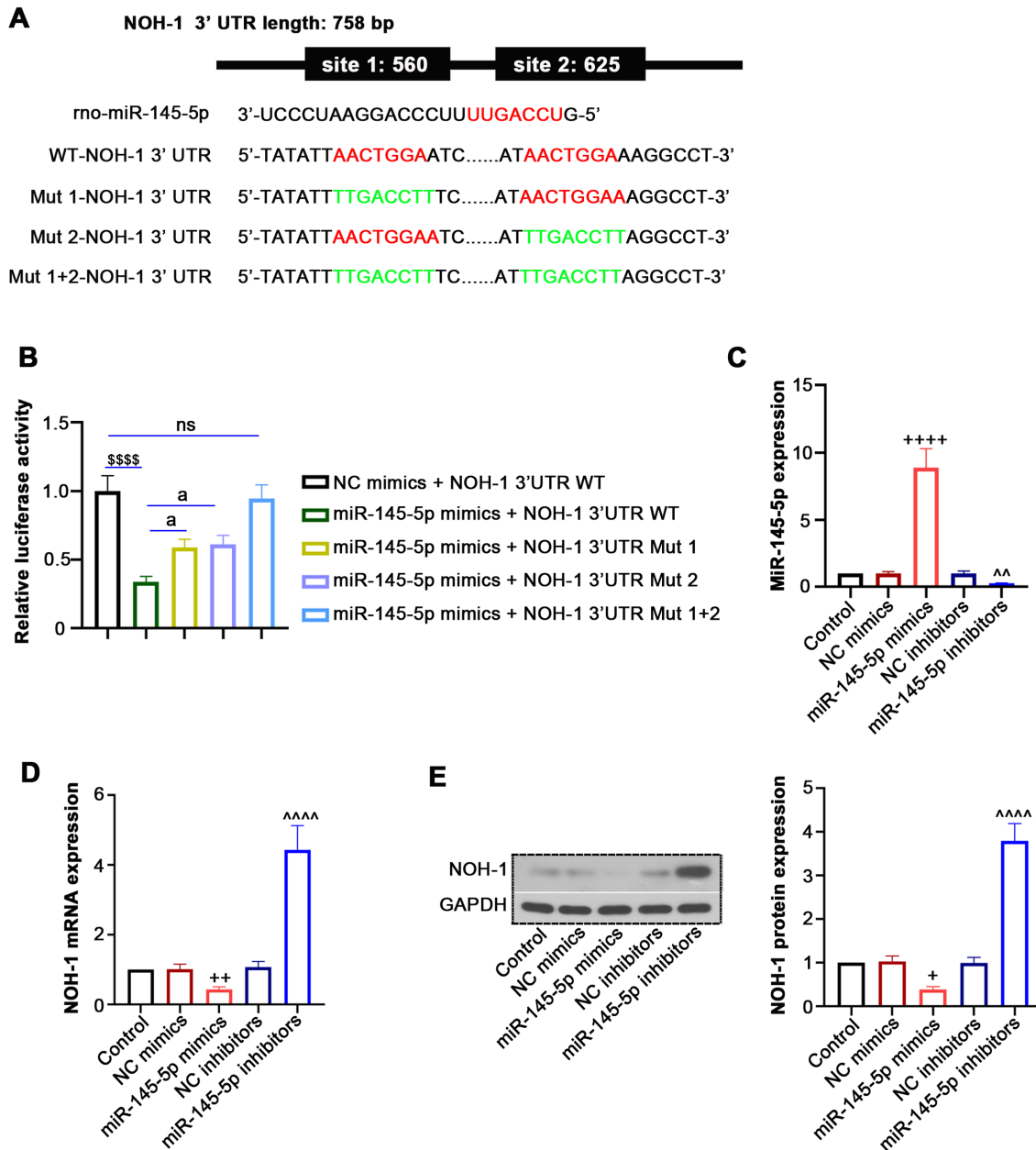


**Fig. 2.** (NADPH) oxidase homolog 1 (NOH-1) is a target for miR-145-5p. To explore the interaction between miR-145-5p and NOH-1, HEK-293T cells were co-transfected with NOH-1 3' untranslated region (UTR) (wild- and mutant-type) and miR-145-5p mimics or negative control (NC) mimics. Then, H9c2 cells were transfected with miR-145-5p mimics, NC mimics, miR-145-5p inhibitors, or NC inhibitors. (A) A schematic diagram is shown for the predicted miR-145-5p binding sites within the 3' UTR of NOH-1. Sequences of candidate binding sites between miR-145-5p and NOH-1 are marked in red, while sequences with the point mutation in the target candidate sites are in green. (B) A luciferase reporter assay was performed to measure the luciferase activity. (C) qRT-PCR was performed to detect the expression of miR-145-5p. (D, E) qRT-PCR and western blot analyses were used to detect the NOH-1 expression at the mRNA and protein levels. All results are presented as means  $\pm$  SD from three independent experiments, and they were analyzed by one-way ANOVA. ns, not significant. \$\$\$\$ $P$ <0.001, compared with NC mimics + NOH-1 3'UTR WT. <sup>a</sup> $P$ <0.05, compared with miR-145-5p mimics + NOH-1 3'UTR WT. ++ $P$ <0.01, compared with NC mimics. ++++ $P$ <0.0001, compared with NC mimics. ^^ $P$ <0.01, compared with NC inhibitors. ^^^ $P$ <0.0001, compared with NC inhibitors.

for 3 h and 24 h, we observed decreased LVESP, EF and FS, increased LVEDP, and increased infarct size, suggesting the damage of cardiac structure and function. NOH-1 is known to be upregulated following reperfusion in the heart [22, 23]. NOH-1 deficiency reduces infarct

size, cardiac remodeling, and apoptosis in late ischaemic preconditioning [24]. Moreover, we found that I/R injury induced a reduction in miR-145-5p expression and an elevation in NOH-1. These findings suggest the hypothesis that miR-145-5p and NOH-1 may play an im-

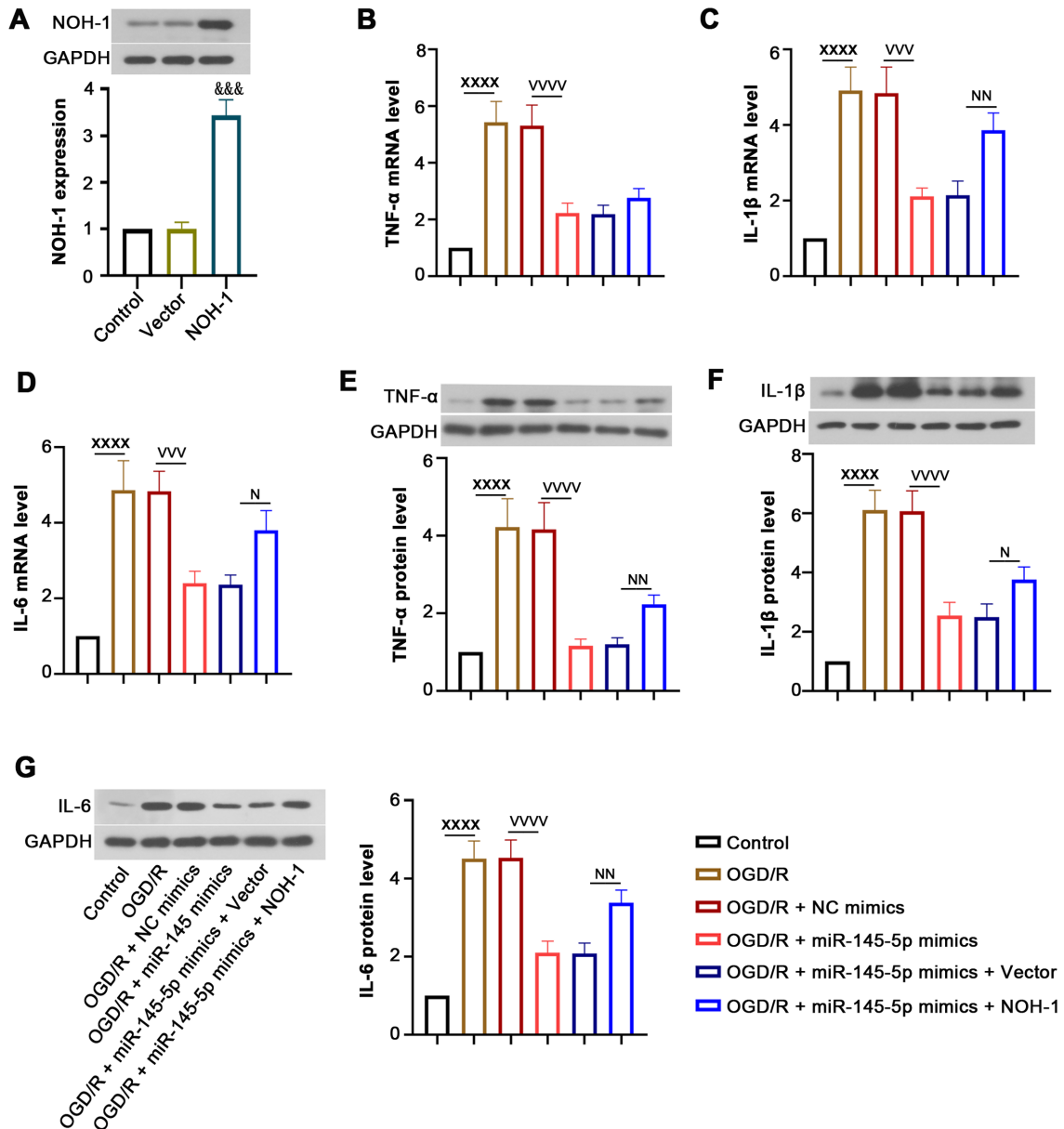


**Fig. 3.** (NADPH) oxidase homolog 1 (NOH-1) promoted the miR-145-5p-related inflammatory response induced by oxygen and glucose deprivation/reperfusion (OGD/R). To investigate the effect of NOH-1 on inflammatory response, H9c2 cells were transfected with miR-145-5p mimics and an NOH-1-overexpressing vector and subjected to OGD/R. (A) Transfection efficiency was determined by western blot assay. (B–G) The mRNA and protein levels of tumor necrosis factor (TNF)- $\alpha$ , IL-1 $\beta$ , and IL-6 were examined by qRT-PCR and western blot analysis. All results are presented as means  $\pm$  SD (n=3). Student's *t*-test was used to evaluate the difference between the empty vector group and the NOH-1-overexpressing plasmid groups. Comparisons of data among multiple groups were conducted with one-way ANOVA. &&&  $P < 0.001$ , compared with empty vector. XXXX  $P < 0.0001$ , compared with Control. VVV  $P < 0.001$ , compared with OGD/R + negative control (NC) mimics. VVVV  $P < 0.0001$ , compared with OGD/R + NC mimics. N  $P < 0.05$ , compared with OGD/R + miR-145-5p mimics + empty vector. NN  $P < 0.01$ , compared with OGD/R + miR-145-5p mimics + empty vector. NNNN  $P < 0.0001$ , compared with OGD/R + miR-145-5p mimics + empty vector.

portant role in myocardial reperfusion injury. On this basis, we explored the relationship between miR-145-5p and NOH-1 and their roles in I/R injury in the OGD/R model established with H9c2 cells. During myocardial I/R injury, a large number of ROS free radicals are produced, and this leads to a severe inflammatory response and apoptosis [25]. Cardiac inflammation due to reperfu-

sion is one of the most important predictors in the process of I/R injury [26]. TNF- $\alpha$  is a well-known pro-inflammatory stimulus that can be triggered in response to I/R injury. It can stimulate the release of other pro-inflammatory cytokines, such as IL-1 $\beta$  and IL-6, further contributing to severe myocardial I/R injury [27–30]. NOH-1, an important molecular link in the regulation of

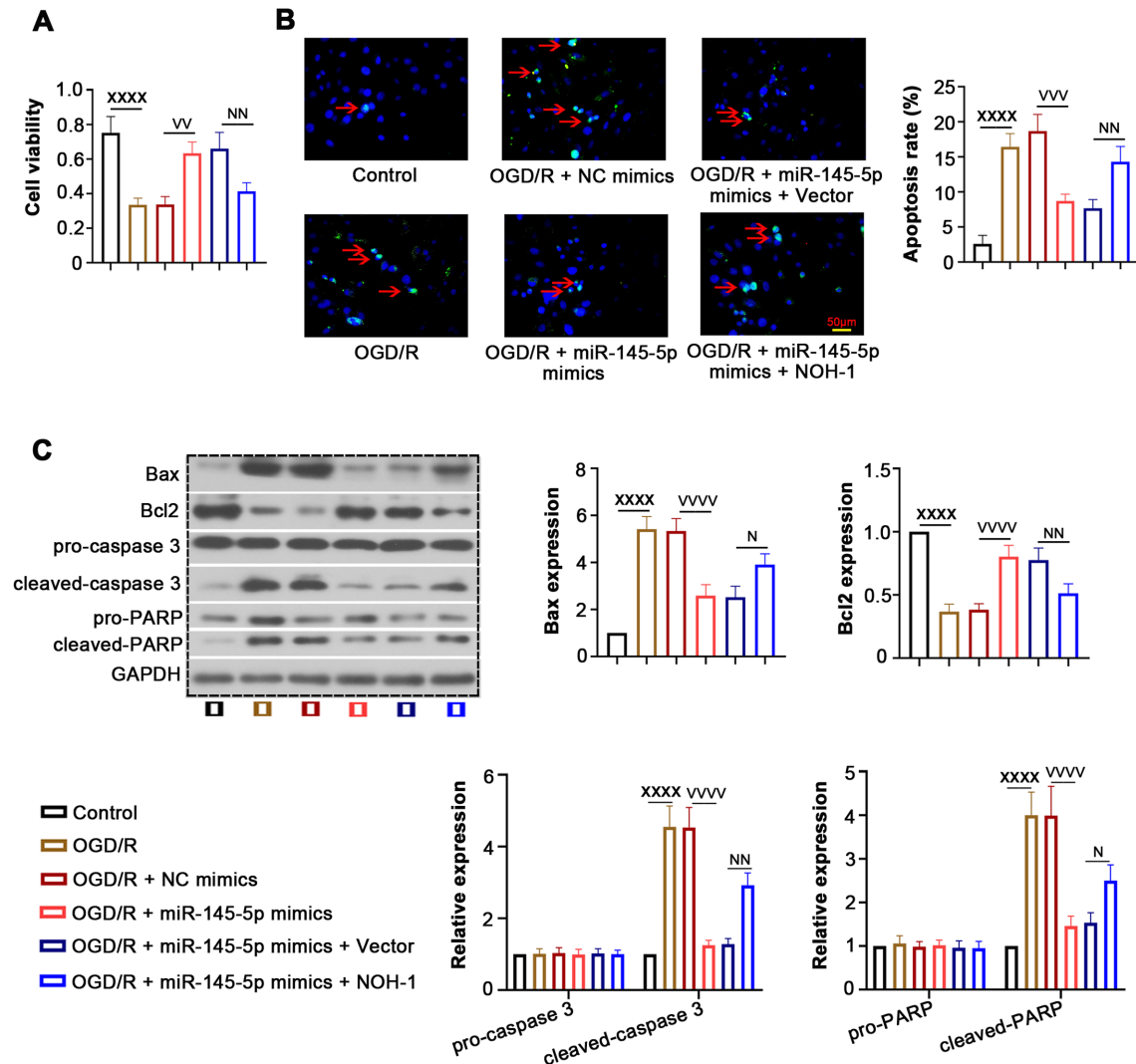


**Fig. 4.** (NADPH) oxidase homolog 1 (NOH-1) increased oxygen and glucose deprivation/reperfusion (OGD/R)-induced cell apoptosis. To evaluate the effect of NOH-1 on cell apoptosis, relevant functional assays were performed. (A) Cell viability was detected using a 3-(4,5-dimethylthiazol-2-yl)-2,5-diphenyltetrazolium bromide (MTT) assay. (B) Cell apoptosis was determined by Terminal deoxynucleotidyl transferase (TdT) dUTP nick-end labeling (TUNEL), and the apoptosis rate was analyzed. (C) Western blot was performed to detect the expression of Bax, Bcl2, pro-caspase-3, cleaved caspase-3, pro-poly(ADP-ribose) polymerase (PARP) and cleaved PARP. All results are presented as means  $\pm$  SD, and they were analyzed by one-way ANOVA. <sup>xxxx</sup> $P < 0.0001$ , compared with the Control. <sup>vv</sup> $P < 0.01$ , compared with OGD/R + negative control (NC) mimics. <sup>vvv</sup> $P < 0.001$ , compared with OGD/R + NC mimics. <sup>vvvv</sup> $P < 0.0001$ , compared with OGD/R + NC mimics. <sup>N</sup> $P < 0.05$ , compared with OGD/R + miR-145-5p mimics + empty vector. <sup>NN</sup> $P < 0.01$ , compared with OGD/R + miR-145-5p mimics + empty vector.

I/R injury, has been reported to play a pivotal role in I/R-induced TNF- $\alpha$  secretion in hepatocytes [31]. The NOH-1 inhibitor has anti-inflammatory effects that prevent lung I/R injury, and this is achieved via the down-regulation of TNF- $\alpha$  and IL-6 [32]. In the current study, we found that miR-145-5p decreased the expression of TNF- $\alpha$ , IL-1 $\beta$ , and IL-6 induced by OGD/R, which was similar to the study of Yuan *et al.* [19]. Upregulation of NOH-1 resulted in a severe inflammatory response, as reflected by the increase in the TNF- $\alpha$ , IL-1 $\beta$ , and IL-6 production, which is in agreement with previous studies. Moreover, NOH-1 was verified to be a direct target of

miR-145-5p. Therefore, the inflammatory effect of NOH-1 on myocardial I/R injury may be modulated by miR-145-5p.

Apoptosis is a major contributor to normal cardiac homeostasis, and obstruction of the apoptotic process leads to serious consequences in the heart [33]. It is well established that the activation of apoptotic signals is closely related to the expression of apoptosis-related signaling molecules [34]. In the process of I/R injury, the pro-apoptotic protein Bax is upregulated, and the anti-apoptotic protein Bcl2 is downregulated [35]. Moreover, both caspase-3 and PARP are the key effectors in

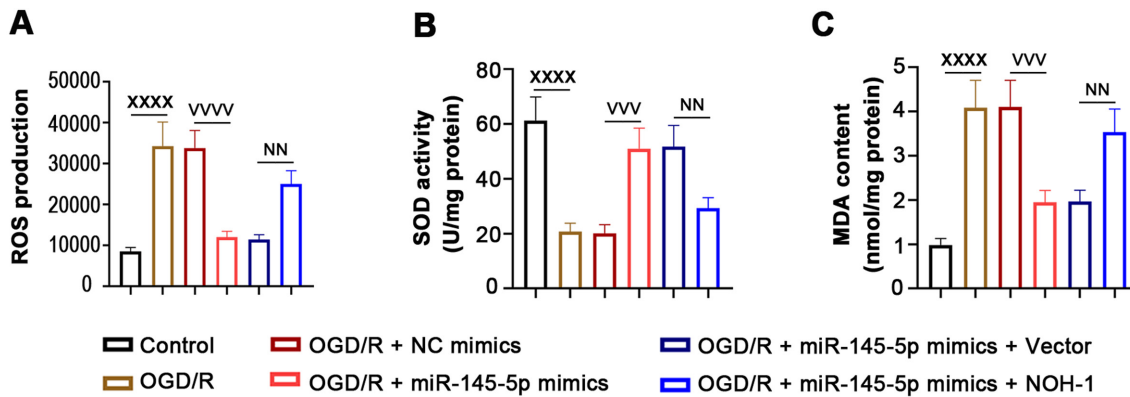


**Fig. 5.** (NADPH) oxidase homolog 1 (NOH-1) aggravated oxygen and glucose deprivation/reperfusion (OGD/R)-induced oxidative stress. Relative levels of the oxidative stress-related parameters reactive oxygen species (ROS), superoxide dismutase (SOD), and malondialdehyde (MDA) were determined using the following methods. (A) ROS production was determined by flow cytometry. (B) SOD activity was examined with an SOD Activity Assay Kit. (C) MDA content was measured with an MDA Assay Kit. All results are presented as means  $\pm$  SD, and they were analyzed by one-way ANOVA. <sup>XXXX</sup> $P < 0.0001$ , compared with the Control. <sup>VVV</sup> $P < 0.001$ , compared with OGD/R + negative control (NC) mimics. <sup>VVVV</sup> $P < 0.0001$ , compared with OGD/R + NC mimics. <sup>NN</sup> $P < 0.01$ , compared with OGD/R + miR-145-5p mimics + empty vector.

the apoptotic pathways [36]. The inactive pro-form of caspase-3 is cleaved, and it subsequently cleaves PARP, eventually triggering the process of apoptosis [37]. In general, downregulation of pro-apoptotic proteins and upregulation of anti-apoptotic proteins can alleviate the apoptotic response. In addition, miR-145-5p has been reported to inhibit apoptosis by decreasing Bax, caspase-3, and caspase-9 and increasing Bcl2 in hypoxia-induced cardiomyocytes [19]. Nevertheless, upregulation of NOH-1 can regulate Bax and Bcl2 expression to induce apoptosis in cardiomyocytes [15, 38]. In our study, we consistently found that miR-145-5p suppressed OGD/R-induced apoptosis and that this was accompanied by a reduction in Bax, cleaved caspase-3 and cleaved PARP and an increase in Bcl2. Interestingly, NOH-1 partially abrogated the above changes, suggesting that miR-145-5p may exert an anti-apoptotic effect through inhibition of NOH-1 in myocardial I/R injury.

Intracellular ROS production is also thought to be a major causative factor for I/R injury [39]. Excessive ROS production eventually leads to cell apoptosis [40]. As reported previously, reperfusion contributes to the occurrence of oxidative stress, which ultimately aggravates the pathological process of I/R injury [41]. SOD is the main enzyme for scavenging ROS [42]. MDA is a marker of lipid peroxidation that reveals the increase of free radical formation after ischemia and indirectly elucidates the degree of cell damage [43]. In a previous study, miR-145-5p is shown to strikingly decrease the production of the oxidative stress factor MDA and increase SOD activity [44]. NOH-1 is a main driver of oxidative stress and induces large amounts of ROS accumulation [38]. In the present study, miR-145-5p overexpression de-

creased ROS generation and the MDA level and elevated SOD antioxidant enzyme activity in OGD/R-treated H9c2 cells, and this was reversed by NOH-1 treatment.

In conclusion, we revealed in this study that miR-145-5p could alleviate the inflammatory response, oxidative stress, and apoptosis via the suppression of NOH-1, thereby ultimately attenuating myocardial I/R injury. Based on our findings, miR-145-5p/NOH-1 may serve as a potential therapeutic target for reperfusion damage in heart.

### Conflict of Interest

The authors declare that there is no conflict of interest.

### Acknowledgments

This study was supported by grants from the Guide Project for Key Research and Development Project of Liaoning Province (grant Nos. 2019010173-JH8/103 and 2017020258-201) and the National Natural Science Foundation of China (grant No. 82001492).

### References

1. Thygesen K, Alpert JS, Jaffe AS, Chaitman BR, Bax JJ, Morrow DA, et al. Executive Group on behalf of the Joint European Society of Cardiology (ESC)/American College of Cardiology (ACC)/American Heart Association (AHA)/World Heart Federation (WHF) Task Force for the Universal Definition of Myocardial Infarction. Fourth universal definition of myocardial infarction (2018). *J Am Coll Cardiol.* 2018; 72: 2231–2264. [Medline] [CrossRef]
2. Dalal H, Evans P, Mourant T, Campbell J, Gray DP. Acute myocardial infarction. *Lancet.* 2003; 361: 2088. [Medline] [CrossRef]

3. Senter S, Francis GS. A new, precise definition of acute myocardial infarction. *Cleve Clin J Med*. 2009; 76: 159–166. [[Medline](#)] [[CrossRef](#)]
4. Lønborg J, Vejstrup N, Kelbæk H, Bøtker HE, Kim WY, Mathiasen AB, et al. Exenatide reduces reperfusion injury in patients with ST-segment elevation myocardial infarction. *Eur Heart J*. 2012; 33: 1491–1499. [[Medline](#)] [[CrossRef](#)]
5. Aboutaleb N, Jamali H, Abolhasani M, Pazoki Toroudi H. Lavender oil (*Lavandula angustifolia*) attenuates renal ischemia/reperfusion injury in rats through suppression of inflammation, oxidative stress and apoptosis. *Biomed Pharmacother*. 2019; 110: 9–19. [[Medline](#)] [[CrossRef](#)]
6. Kalogeris T, Baines CP, Krenz M, Korthuis RJ. Cell biology of ischemia/reperfusion injury. *Int Rev Cell Mol Biol*. 2012; 298: 229–317. [[Medline](#)] [[CrossRef](#)]
7. Braunersreuther V, Montecucco F, Asrih M, Pelli G, Galan K, Frias M, et al. Role of NADPH oxidase isoforms NOX1, NOX2 and NOX4 in myocardial ischemia/reperfusion injury. *J Mol Cell Cardiol*. 2013; 64: 99–107. [[Medline](#)] [[CrossRef](#)]
8. Zhang G, Zhang F, Muh R, Yi F, Chalupsky K, Cai H, et al. Autocrine/paracrine pattern of superoxide production through NAD(P)H oxidase in coronary arterial myocytes. *Am J Physiol Heart Circ Physiol*. 2007; 292: H483–H495. [[Medline](#)] [[CrossRef](#)]
9. Lakhan SE, Kirchgessner A, Hofer M. Inflammatory mechanisms in ischemic stroke: therapeutic approaches. *J Transl Med*. 2009; 7: 97. [[Medline](#)] [[CrossRef](#)]
10. Yang Y, Rosenberg GA. Blood-brain barrier breakdown in acute and chronic cerebrovascular disease. *Stroke*. 2011; 42: 3323–3328. [[Medline](#)] [[CrossRef](#)]
11. Xiong F, Xiao D, Zhang L. Norepinephrine causes epigenetic repression of PKCε gene in rodent hearts by activating Nox1-dependent reactive oxygen species production. *FASEB J*. 2012; 26: 2753–2763. [[Medline](#)] [[CrossRef](#)]
12. Tong XX, Wu D, Wang X, Chen HL, Chen JX, Wang XX, et al. Ghrelin protects against cobalt chloride-induced hypoxic injury in cardiac H9c2 cells by inhibiting oxidative stress and inducing autophagy. *Peptides*. 2012; 38: 217–227. [[Medline](#)] [[CrossRef](#)]
13. Choi H, Stark RJ, Raja BS, Dikalova A, Lamb FS. Apoptosis signal-regulating kinase 1 activation by Nox1-derived oxidants is required for TNFα receptor endocytosis. *Am J Physiol Heart Circ Physiol*. 2019; 316: H1528–H1537. [[Medline](#)] [[CrossRef](#)]
14. Zeng SY, Yang L, Yan QJ, Gao L, Lu HQ, Yan PK. Nox1/4 dual inhibitor GKT137831 attenuates hypertensive cardiac remodelling associating with the inhibition of ADAM17-dependent proinflammatory cytokines-induced signalling pathways in the rats with abdominal artery constriction. *Biomed Pharmacother*. 2019; 109: 1907–1914. [[Medline](#)] [[CrossRef](#)]
15. Matsuno K, Iwata K, Matsumoto M, Katsuyama M, Cui W, Murata A, et al. NOX1/NADPH oxidase is involved in endotoxin-induced cardiomyocyte apoptosis. *Free Radic Biol Med*. 2012; 53: 1718–1728. [[Medline](#)] [[CrossRef](#)]
16. Quiat D, Olson EN. MicroRNAs in cardiovascular disease: from pathogenesis to prevention and treatment. *J Clin Invest*. 2013; 123: 11–18. [[Medline](#)] [[CrossRef](#)]
17. Selbach M, Schwanhäusser B, Thierfelder N, Fang Z, Khanin R, Rajewsky N. Widespread changes in protein synthesis induced by microRNAs. *Nature*. 2008; 455: 58–63. [[Medline](#)] [[CrossRef](#)]
18. Liu Z, Tao B, Fan S, Pu Y, Xia H, Xu L. MicroRNA-145 Protects against myocardial ischemia reperfusion injury via CAMKII-mediated antiapoptotic and anti-inflammatory pathways. *Oxid Med Cell Longev*. 2019; 2019: 8948657. [[Medline](#)] [[CrossRef](#)]
19. Yuan M, Zhang L, You F, Zhou J, Ma Y, Yang F, et al. MiR-145-5p regulates hypoxia-induced inflammatory response and apoptosis in cardiomyocytes by targeting CD40. *Mol Cell Biochem*. 2017; 431: 123–131. [[Medline](#)] [[CrossRef](#)]
20. Wu G, Tan J, Li J, Sun X, Du L, Tao S. miRNA-145-5p induces apoptosis after ischemia-reperfusion by targeting dual specificity phosphatase 6. *J Cell Physiol*. 2019; 234: 16281–16289. [[Medline](#)] [[CrossRef](#)]
21. Yang Y, Zhao L, Ma J. Penhexyclidine hydrochloride preconditioning provides cardiac protection in a rat model of myocardial ischemia/reperfusion injury via the mechanism of mitochondrial dynamics mechanism. *Eur J Pharmacol*. 2017; 813: 130–139. [[Medline](#)] [[CrossRef](#)]
22. Yang Q, Wu W, Li Q, Chen C, Zhou R, Qiu Y, et al. High-dose polymerized hemoglobin fails to alleviate cardiac ischemia/reperfusion injury due to induction of oxidative damage in coronary artery. *Oxid Med Cell Longev*. 2015; 2015: 125106. [[Medline](#)] [[CrossRef](#)]
23. Morimoto H, Hirose M, Takahashi M, Kawaguchi M, Ise H, Kolattukudy PE, et al. MCP-1 induces cardioprotection against ischaemia/reperfusion injury: role of reactive oxygen species. *Cardiovasc Res*. 2008; 78: 554–562. [[Medline](#)] [[CrossRef](#)]
24. Jiang S, Streeter J, Schickling BM, Zimmerman K, Weiss RM, Miller FJ Jr. Nox1 NADPH oxidase is necessary for late but not early myocardial ischaemic preconditioning. *Cardiovasc Res*. 2014; 102: 79–87. [[Medline](#)] [[CrossRef](#)]
25. Malhi H, Gores GJ, Lemasters JJ. Apoptosis and necrosis in the liver: a tale of two deaths? *Hepatology*. 2006; 43:(Suppl 1): S31–S44. [[Medline](#)] [[CrossRef](#)]
26. Zahler S, Massoudy P, Hartl H, Hähnel C, Meisner H, Becker BF. Acute cardiac inflammatory responses to postischemic reperfusion during cardiopulmonary bypass. *Cardiovasc Res*. 1999; 41: 722–730. [[Medline](#)] [[CrossRef](#)]
27. Fang L, Moore XL, Dart AM, Wang LM. Systemic inflammatory response following acute myocardial infarction. *J Geriatr Cardiol*. 2015; 12: 305–312. [[Medline](#)]
28. Huang WC, Chou RH, Chang CC, Hsu CY, Ku YC, Huang HF, et al. Systemic inflammatory response syndrome is an independent predictor of one-year mortality in patients with acute myocardial infarction. *Zhonghua Minguo Xinzangxue Hui Zazhi*. 2017; 33: 477–485. [[Medline](#)]
29. Saha P, Smith A. TNF-α (Tumor Necrosis Factor-α). *Arterioscler Thromb Vasc Biol*. 2018; 38: 2542–2543. [[Medline](#)] [[CrossRef](#)]
30. Ahn J, Kim J. Mechanisms and consequences of inflammatory signaling in the myocardium. *Curr Hypertens Rep*. 2012; 14: 510–516. [[Medline](#)] [[CrossRef](#)]
31. Spencer NY, Zhou W, Li Q, Zhang Y, Luo M, Yan Z, et al. Hepatocytes produce TNF-α following hypoxia-reoxygenation and liver ischemia-reperfusion in a NADPH oxidase- and c-Src-dependent manner. *Am J Physiol Gastrointest Liver Physiol*. 2013; 305: G84–G94. [[Medline](#)] [[CrossRef](#)]
32. Cui Y, Wang Y, Li G, Ma W, Zhou XS, Wang J, et al. The Nox1/Nox4 inhibitor attenuates acute lung injury induced by ischemia-reperfusion in mice. *PLoS One*. 2018; 13: e0209444. [[Medline](#)] [[CrossRef](#)]
33. Li X, Ren Y, Sorokin V, Poh KK, Ho HH, Lee CN, et al. Quantitative profiling of the rat heart myoblast secretome reveals differential responses to hypoxia and re-oxygenation stress. *J Proteomics*. 2014; 98: 138–149. [[Medline](#)] [[CrossRef](#)]
34. Xu P, Cai X, Zhang W, Li Y, Qiu P, Lu D, et al. Flavonoids of *Rosa roxburghii* Tratt exhibit radioprotection and anti-apoptosis properties via the Bcl-2(Ca(2+))/Caspase-3/PARP-1 pathway. *Apoptosis*. 2016; 21: 1125–1143. [[Medline](#)] [[CrossRef](#)]
35. Wang YQ, Tang YF, Yang MK, Huang XZ. Dexmedetomidine alleviates cerebral ischemia-reperfusion injury in rats via inhibition of hypoxia-inducible factor-1α. *J Cell Biochem*. 2018; 120: 7834–7844.
36. Cao ZH, Yin WD, Zheng QY, Feng SL, Xu GL, Zhang KQ. Caspase-3 is involved in IFN-γ- and TNF-α-mediated MIN6 cells apoptosis via NF-κB/Bcl-2 pathway. *Cell Biochem Biophys*. 2013; 67: 1239–1248. [[Medline](#)] [[CrossRef](#)]
37. Perchellet EM, Wang Y, Weber RL, Sperfsilage BJ, Lou K,

- Crossland J, et al. Synthetic 1,4-anthracenedione analogs induce cytochrome c release, caspase-9, -3, and -8 activities, poly(ADP-ribose) polymerase-1 cleavage and internucleosomal DNA fragmentation in HL-60 cells by a mechanism which involves caspase-2 activation but not Fas signaling. *Biochem Pharmacol.* 2004; 67: 523–537. [[Medline](#)] [[CrossRef](#)]
38. Zanetti F, Giacomello M, Donati Y, Carnesecchi S, Frieden M, Barazzone-Argiroffo C. Nicotine mediates oxidative stress and apoptosis through cross talk between NOX1 and Bcl-2 in lung epithelial cells. *Free Radic Biol Med.* 2014; 76: 173–184. [[Medline](#)] [[CrossRef](#)]
39. De Silva TM, Brait VH, Drummond GR, Sobey CG, Miller AA. Nox2 oxidase activity accounts for the oxidative stress and vasomotor dysfunction in mouse cerebral arteries following ischemic stroke. *PLoS One.* 2011; 6: e28393. [[Medline](#)] [[CrossRef](#)]
40. Bai SC, Xu Q, Li H, Qin YF, Song LC, Wang CG, et al. NADPH Oxidase Isoforms Are Involved in Glucocorticoid-Induced Preosteoblast Apoptosis. *Oxid Med Cell Longev.* 2019; 2019: 9192413. [[Medline](#)] [[CrossRef](#)]
41. Luo SY, Li R, Le ZY, Li QL, Chen ZW. Anfibatide protects against rat cerebral ischemia/reperfusion injury via TLR4/JNK/caspase-3 pathway. *Eur J Pharmacol.* 2017; 807: 127–137. [[Medline](#)] [[CrossRef](#)]
42. Ciancarelli I, Di Massimo C, De Amicis D, Pistarini C, Tozzi Ciancarelli MG. Uric acid and Cu/Zn superoxide dismutase: potential strategies and biomarkers in functional recovery of post-acute ischemic stroke patients after intensive neurorehabilitation. *Curr Neurovasc Res.* 2015; 12: 120–127. [[Medline](#)] [[CrossRef](#)]
43. Mishra S, Mishra BB. Study of Lipid Peroxidation, Nitric Oxide End Product, and Trace Element Status in Type 2 Diabetes Mellitus with and without Complications. *Int J Appl Basic Med Res.* 2017; 7: 88–93. [[Medline](#)] [[CrossRef](#)]
44. Yu C, Liu Y, Sun L, Wang D, Wang Y, Zhao S, et al. Chronic obstructive sleep apnea promotes aortic remodeling in canines through miR-145/Smad3 signaling pathway. *Oncotarget.* 2017; 8: 37705–37716. [[Medline](#)] [[CrossRef](#)]